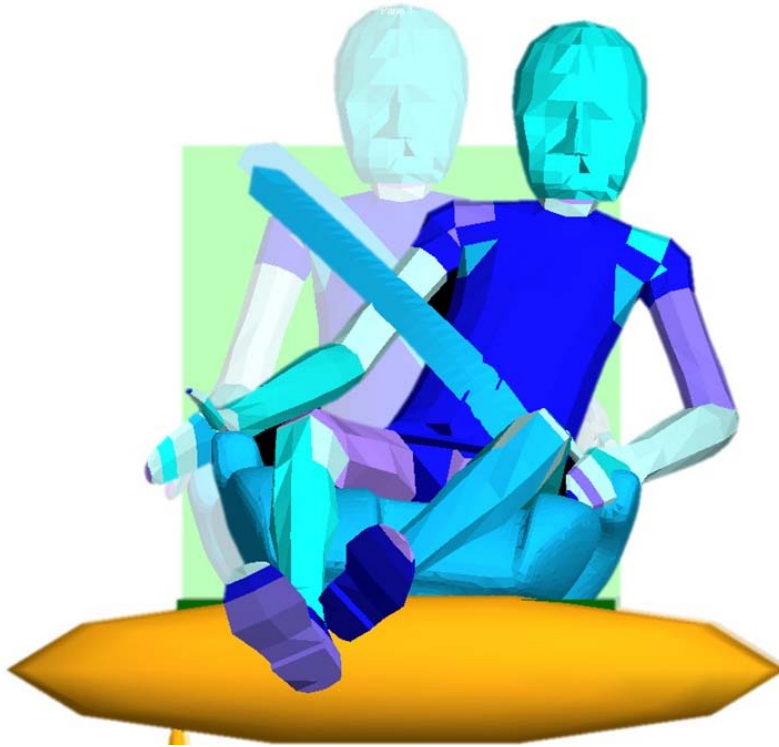




**CHALMERS**  
UNIVERSITY OF TECHNOLOGY

---



# **Enhancing a Multibody Model of a 6-year-old Controller Implementation**

Master's thesis in the ERASMUS programme

**RAMIRO GARCÍA GALÁN**



MASTER'S THESIS IN THE ERASMUS PROGRAMME

# Enhancing a Multibody Model of a 6-year-old

Controller Implementation

RAMIRO GARCÍA GALÁN

Department of Applied Mechanics  
Division of Vehicle Safety  
CHALMERS UNIVERSITY OF TECHNOLOGY  
Göteborg, Sweden 2015

Enhancing a Multibody Model of a 6-year-old  
Controller Implementation  
RAMIRO GARCÍA GALÁN

© RAMIRO GARCÍA GALÁN, 2015

Master's Thesis 2015:84  
ISSN 1652-8557  
Department of Applied Mechanics  
Division of Vehicle Safety  
Chalmers University of Technology  
SE-412 96 Göteborg  
Sweden  
Telephone: + 46 (0)31-772 1000

Cover:  
Front view of the active 6-year-old HBM in MADYMO code (TASS, Rijswijk, the Netherlands) sitting in a booster and restraint with a 3-point seatbelt.  
Name of the printers / Department of Applied Mechanics  
Göteborg, Sweden 2015-03-03

Enhancing a Multibody Model of a 6-year-old  
Controller Implementation  
Master's thesis in Master's in the ERASMUS programme  
RAMIRO GARCÍA GALÁN  
Department of Applied Mechanics  
Division of Vehicle Safety  
Chalmers University of Technology

## **Abstract**

The number of children injured or disabled each year as a result of road traffic crashes has been estimated at around 10 millions around the world. Avoiding those fatalities and protecting car occupants are a goal many researchers are actively working toward. One of the fields involved in this effort is the modelling of the behavior of the human body (HBM) in pre-crash and crash situations using computer-aided simulations. The aim of this study is to improve an active 6-year-old HBM with more realistic and biofidelic movements to understand its behavior in pre-crash events. More specifically, steering events will be analyzed.

The thesis at hand recreates a child's movements using a HBM modelled in MADYMO. The active 6-year-old HBM consists of an active spine, which is necessary to keep the body in an upright position during long simulations. Rigid bodies simulate the vertebrae of the spine and the addition of controllers implemented in the joints between the vertebrae maintains the HBM's posture. The first step to improve the model was testing different reference systems for measuring vertebral angles. When these reference systems were defined, it was taken into account how the body moves trying to keep the balance. Secondly, the sensitivity of the spinal gains was studied to understand how it affected the movement of the active 6-year-old HBM when loaded with a lateral acceleration.

The results point to the fact that the gains for lateral bending for the cervical, thoracic and lumbar spine were the most influential when a lateral acceleration was applied. In addition to that, it was revealed that the model for which all spinal joints are measured by taking the vertebral angles relative to the global coordinate system, fits in the volunteer corridors. Hence, this model can be useful to evaluate child restraint systems. However, further validations compared to other experimental data and with other child restraints are recommended. In addition to that, an improved model of the 6-year-old HBM – after further validation- could be used to optimize restraints and for seat assessment.

## **Acknowledgements**

The work presented in this report was carried out at SAFER, the Vehicle Traffic Safety Centre at Chalmers, Gothenburg, Sweden.

THANK YOU Karin and Jonas, because with your help and your time have made this project is done.

THANK YOU people from SAFER, especially Alba and Pooja, because you have taught me many things in these months.

THANK YOU everyone that helped me with this project (Jakob, Erick, Nacho, Jona...), because everything was very useful.

THANK YOU Ramiro, Carmen, Laura, because your support has made finally I get it.

THANK YOU friends of my university, because sharing suffering creates strong bonds of friendship.

THANK YOU friends of my Erasmus, because an intense year always marks.

THANK YOU old Friends, because you never let me down.

Just...THANKS!

# Contents

|   |     |
|---|-----|
| Abstract .....                                  | I   |
| Acknowledgements .....                          | II  |
| Contents.....                                   | III |
| 1 Introduction.....                             | 1   |
| 1.1 Purpose.....                                | 1   |
| 1.2 Limitations .....                           | 1   |
| 2 Background.....                               | 2   |
| 2.1 Anatomy of children.....                    | 2   |
| 2.2 PID Controller .....                        | 3   |
| 3 Experimental data.....                        | 4   |
| 3.1 Methodology.....                            | 4   |
| 3.2 Active 6-Year-Old HBM.....                  | 5   |
| 4 Method .....                                  | 8   |
| 4.1 Simulation.....                             | 8   |
| 4.2 Sensitivity .....                           | 11  |
| 5 Results.....                                  | 13  |
| 5.1 Simulation.....                             | 13  |
| 5.1.1 Active 6-year-old HBM version 32.....     | 13  |
| 5.1.2 Head and upper sternum displacements..... | 14  |
| 5.1.3 Kinematic responses.....                  | 14  |
| 5.2 Sensitivity .....                           | 17  |
| 6 Discussion.....                               | 19  |
| 7 Conclusion .....                              | 23  |
| 8 Future Work .....                             | 24  |
| 9 References .....                              | 25  |
| 10 Appendix.....                                | 27  |
| 10.1 Appendix A.....                            | 27  |

# Notations

**FE** Finite Element(s)

**PID** Proportional-Integral-Derivative

**HBM** Human Body Model

**6YO HBM** 6-year-old facet occupant multi-body model in the MADYMO code (TASS, Rijswijk, the Netherlands) [14]

**Active 6-year-old HBM** the 6YO HBM with an active spine

**MADYMO** A software for analyzing and optimizing occupant safety design (TASS, Rijswijk, the Netherlands) [1]

**KC** Gains corresponding with the cervical spine for flexion-extension movement

**KC\_lat** Gains corresponding with the cervical spine for lateral bending

**KC\_rot** Gains corresponding with the cervical spine for rotation

**KT** Gains corresponding with the thoracic spine for flexion-extension movement

**KT\_lat** Gains corresponding with the thoracic spine for lateral bending

**KT\_rot** Gains corresponding with the cervical spine for rotation

**KL** Gains corresponding with the lumbar spine for flexion-extension movement

**KL\_lat** Gains corresponding with the lumbar spine for lateral bending

**KL\_rot** Gains corresponding with the cervical spine for rotation

**NasionY\_match** Displacement for nasion node in Y-axis

**NasionZ\_match** Displacement for nasion node in Z-axis

**SternumY\_match** Displacement for sternum node in Y-axis

**SternumZ\_match** Displacement for sternum node in Z-axis

# 1 Introduction

In the WHO European Region, road crashes kill annually 92,000 people and 2.4 million are heavily injured and required hospital attention [2]. Road traffic injuries are the leading cause of death for those aged 5-29[2]. Nowadays, there are 111 countries in the entire world with seat-belt laws and 96 countries with child-restraint system laws (these restrain systems together with seat belts have reduced the risk of fatal injuries between a 54% and an 80%) to protect rear-seat car occupants [3].

Therefore, the kinematics and behavior of children in different events and with different restraint systems is a field where there is room for extensive research, e.g. on the role of the shoulder belt position of the child when the car performs an evasive event [4] [5], the effect of the booster seat design on children's [6], etcetera.

## 1.1 Purpose

This thesis seeks to explore controller parameters to understand how they affect an active 6-year-old HBM's [7, 8] kinematics response compared to the volunteer data for emergency events [4] and [5]. In order to address the essential questions underlying this project, research efforts focused on two different things. On the one hand, the definition of the controller reference angle; on the other hand, a careful study of the sensitivity of the gains themselves, in the course of steering events, and the resulting impact on the behavior of the active 6-year-old HBM.

## 1.2 Limitations

The work does not involve any change in the properties of the elements – or the values of the gains – of the active 6-year-old HBM [7]. This means that the work of this thesis based on version 32 [8] (see Table 1) of this model. While different settings were tested, this had no impact on the HBM version used.

The models resulting from this research were compared with the behavior of the children reflected in the experimental data for the steering event [4]. While it is important to know that the number of children tested cannot represent the behavior of all children, the figures that derive from that piece of research represent a biofidelic approximation to predict the approximate behavior of a child in different events.

In order to study the sensitivity gains, an optimization method was chosen. While there are other methods that could have been used an optimization method seemed appropriate in this case. The main reason for this was that the software program required for this project produced, as part of its optimization process, gain sensitivity output. Thus, even though optimization data output was largely ignored – due to its irrelevance for this study, - the sought data was not optimization output *per se*; it was the gain sensitivity data output produced as part of the program's optimization settings.

## 2 Background

### 2.1 Anatomy of children

The human anatomy undergoes a variety of changes from birth to adulthood. This is shown in the Fig. 1 and reported in [9]. For example, the head of a newborn is a quarter of the total length of that of an adult but is heavier relative to the total size and weight of the body [9]. Likewise, the mid-point of the body for the newborns is above the navel. However, when the body grows up, the point is displaced down until it is situated near the pubic symphysis for a 16-year-old [9].

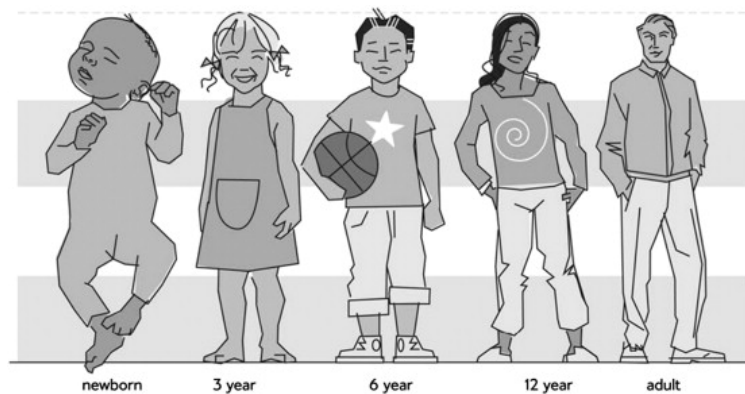


Fig. 1 The proportional changes in body segments with age as reported by [9]. Copyright Volvo Cars.

In a 6-year-old child the neck is still developing, since muscle strength is increasing. Cervical facets are predominantly horizontal (less than in the case of a newborn) [10]. Due to differences in relative size and weight such as the mentioned above, lateral and/or longitudinal car acceleration will affect children and adults differently, causing a larger head and spine displacement in children [11].

In crash accidents, the majority of the load exerted on the body by the seatbelt is applied to the chest. This is called the thorax and is composed of the rib cage, the sternum and the thoracic vertebral column. This structure is very stiff in the adult age; however, it undergoes a stiffening process that lasts up to puberty. During childhood, the sternum and the exterior of the rib are composed of cartilage, which is progressively calcified until its full development [12]. During this phase, the load applied to the chest by the seatbelt creates more deflection, which may lead to internal organ injuries, and a higher chest compression compared to adults [11].

The pelvis has an important function for passenger safety. Together with the clavicle and the sternum, the pelvis works as an anchor for the 3 points seatbelt. They are the stiffest parts of the middle and upper part of the body, absorbing the load created by the belt. Most parts of the pelvis are cartilaginous in newborns, and progressively ossify until the age of 8 years [12]. Moreover, the iliac spines, the part of the pelvis that ideally will stop the seatbelt from sliding on to the soft abdomen, are not completely developed until puberty [12].

## 2.2 PID Controller

Proportional, Integral and Derivative (PID) controllers are control loop feedback mechanisms. The purpose of these controllers is to minimize an error that is calculated by finding the difference between the value of a measured process variable and a desired set point (Fig. 2). Three constant parameters can be adjusted:

- The Proportional gain constant ( $K_p$ ): scales the current error value.
- The Integral gain constant ( $T_i$ ): scales linearly the accumulation of past errors; the output is proportional to both the magnitude and the size of the error.
- The Derivational gain constant ( $T_d$ ): scales the future error. When there is a change in the absolute value of the error, it tries to maintain the error at the minimum value and controls it at the same velocity it is produced.

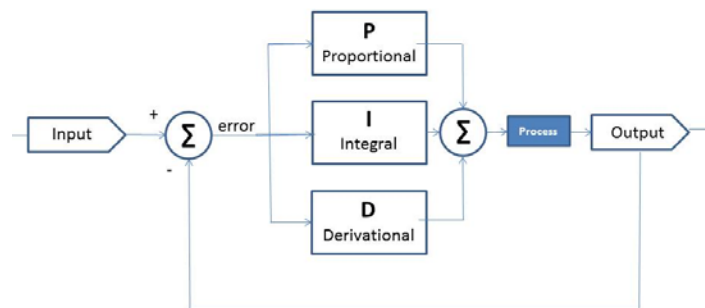


Fig. 2 Basic PID controller scheme taken from [13]

The PID controllers used in the model for this thesis were the ideal PID controller for a Single Input Single Output. It can be expressed in the frequency domain as:

$$U(s) = G_c(s) E(s) \quad (2.2.1)$$

$$G_c(s) = K_p \left( 1 + \frac{1}{T_i s} + T_d s \right) \quad (2.2.2)$$

This form has the proportional gain ( $K_p$ ), the integral time ( $T_i$ ) and the derivative time ( $T_d$ ).

PID controllers have been applied to human modelling to simulate active muscle behavior in pre-crash and in-crash events. For example, an active adult model was designed by Cappon [14].

## 3 Experimental data

### 3.1 Methodology

In order to understand the child's kinematic response when the car does a sharp movement, Stockman et al. [5] and Bohman et al. [4] performed a study of the kinematics of child occupants when the driver does emergency events: evasive steering and braking. They focused on the motion of the upper torso and the seat belt position relative to the shoulder (Fig. 3).



*Fig. 3 Left figure shows the data video obtained in the steering event [4], while the figure in the right shows the braking event [5].*

For their studies, they included 16 children divided in two groups, based on stature, short children (107-123 cm) and tall children (135-150 cm). Both groups were restrained with the seat belt and with an extra restraint system; the first group was tested with a booster cushion with no backrest and a high back booster seat, while the second one was tested with a booster cushion with no backrest and just with the seat belt. In both tests, the children were seated on the right side of the rear seat while four cameras recorded their movements.

To perform the braking event, the vehicle was driving straight with a velocity of 70 km/h and the driver hit the brake until the car stopped [5], achieving a negative acceleration of approximately 1.0 g. (Fig. 4). During the steering event, the vehicle had a constant velocity of 50 km/h when it was turned sharply to the right in a curve with 14-m radius [4]. The maximum lateral acceleration achieved was 0.8 g. (Fig.4).

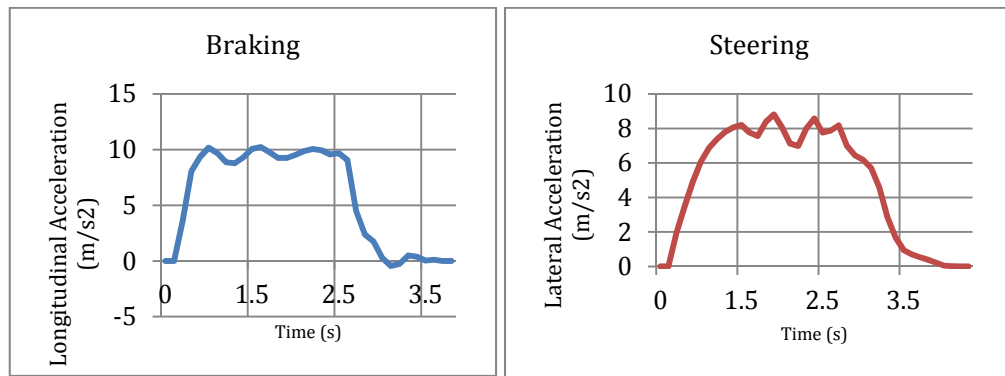


Fig. 4 Acceleration achieved for the braking (left) and steering event (right) events.

In the steering event study, the authors concluded that for the shorter children the belt slipped off in the majority of turns when they were seated in the booster with no backrest (Fig. 3). At the same time, the taller group shows that the belt remained in the shoulder in both test situations [4].

### 3.2 Active 6-Year-Old HBM

Numerical child models can be used for child safety research and to gain a deeper understanding of child biomechanics. In simulations of long-duration events, the 6 year-old facet occupant multi-body model (6YO HBM) in the MADYMO code (TASS, Rijswijk, the Netherlands) [15] would require postural stability. The first version of the active 6-year-old HBM was created by Gras and Brodin [16-17, 8] with the same modelling strategy as used by Cappon [14] for a 50<sup>th</sup> percentile male pedestrian model. They implemented a stabilizing behavior into the 6YO HBM adding torque actuators in the human spine. This chapter describes the development of the active 6-year-old HBM [8]. The spine is composed of 25 rigid bodies simulating the vertebrae that are connected by kinematic joints. Torque actuators apply a torque in the spinal joints, representing muscle activity, and were controlled by PID controllers. The controller gains were based on adult data and scaled by 50% for a first version of the active child model [16-17]. The model was seated on a booster cushion and loaded with the average experimental pulse from [4] and [5].

In the active 6-year-old HBM [8], sensors measure the angles formed by the difference between the current position of the vertebrae and the initial reference posture, providing an error to the PID controller. All controllers provide data to transform the information from the sensor into a torque. A torque was applied to each joint to correct the error, including the joints between the pelvis and the hip, pelvis and lower spine and in between the head and the top of the spine. The chart in Fig. 5 shows the flow of the action.

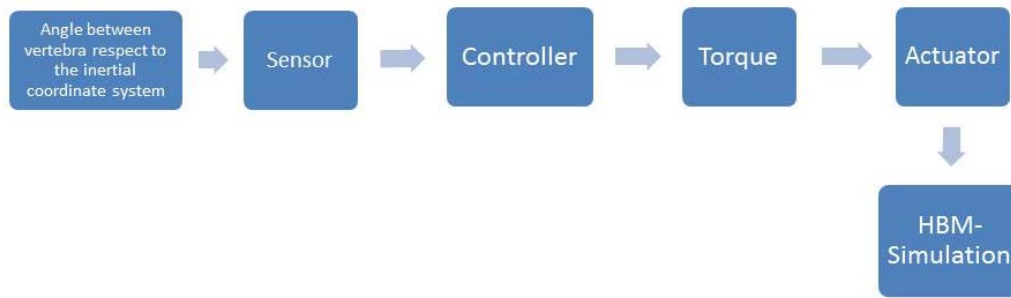


*Fig. 5 Illustration of the control implementation for each joint in the active 6-year-old model [8]. The controller analyzes the angle measure by the sensor, the controller determines the size of the torque and the actuator applies the torque in the HBM simulation..*

There are three different types of torque applied to the spine of the active 6-year-old model [8]; the first one is a static torque, which keeps the model upright. The second one depends on the mass of each vertebra ( $m_n$ ), the distance ( $l$ ), the gravity force ( $g$ ) and the angle between the vertebra and the initial reference ( $\varphi$ ), where “n” denotes the different vertebrae and small angles are considerate as Equation 3.1 shows and Fig. 6. The last one is a dynamic torque that creates a motion to return the model to the original position.

$$T_n = \text{Sum}(m_n) * l * g * \varphi \quad (3.1)$$

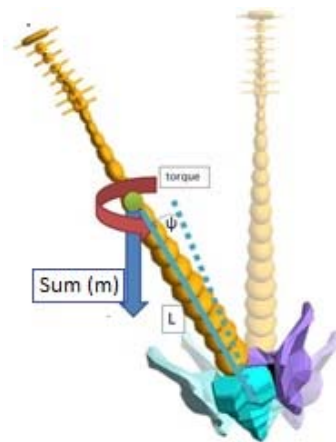


*Fig. 6 Illustration of how the torque is created. The mass of each vertebra together with the gravity generates a force directed toward the ground. This force is multiplied by the distances between the reference point and the angle that the sensor collected in each axis, creating the torque that counteracts the external accelerations that caused the model movement, e.g. gravity, lateral acceleration, braking force, etcetera.*

The active 6-year-old HBM developed by Gras and Brodin [16-17] was improved by Brodin et al. [8] (Fig. 7) by adding controllers for each of the three rotational degrees of freedom in the spine: flexion-extension, lateral bending and rotation. Therefore, each joint has three gains that can be tuned for each rotational degree of freedom. To simplify, the joints were grouped in three groups (cervical, thoracic, and lumbar) with identical controller gains within the groups.

This thesis uses the active 6-year-old HBM Version 32 [17] (see Table 1). The most recent version of the active 6-year-old HBM was developed by Brodin et

al. [7], in which the gains and the inertial coordinate system were modified with respect to version 32 [8] (see Table 1).

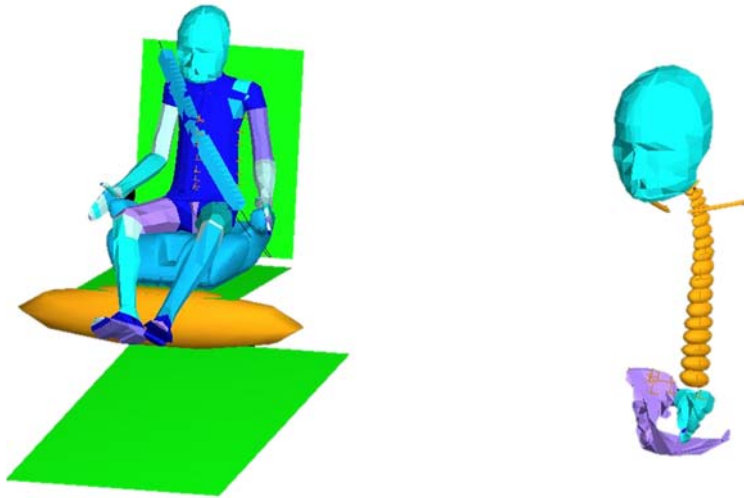


*Fig. 7 Active 6-year-old HBM [8] loaded by gravity force*

## 4 Method

### 4.1 Simulation

All simulations were performed with the MADYMO code (v. 7.4.1) (TASS, Rijswijk, the Netherlands) [1]. The pulse of the steering event has a duration of 4 s. However, all simulations were performed with a duration of 1.6 s, hence only the beginning of the steering event was simulated. For the first 0.5s, only gravity loading was applied, to position the active 6-year-old HBM. After that, additional lateral acceleration from the steering event [4] was applied (Fig. 8).

Data was pre-processed using XMADgic (version 7.4.1) (TASS, Rijswijk, the Netherlands). The software used to post-process the data were: Matlab (v. R2010b) (The MathWorks, Inc., Massachusetts, USA) and XPost (v. 7.4.1) (TASS, Rijswijk, the Netherlands).

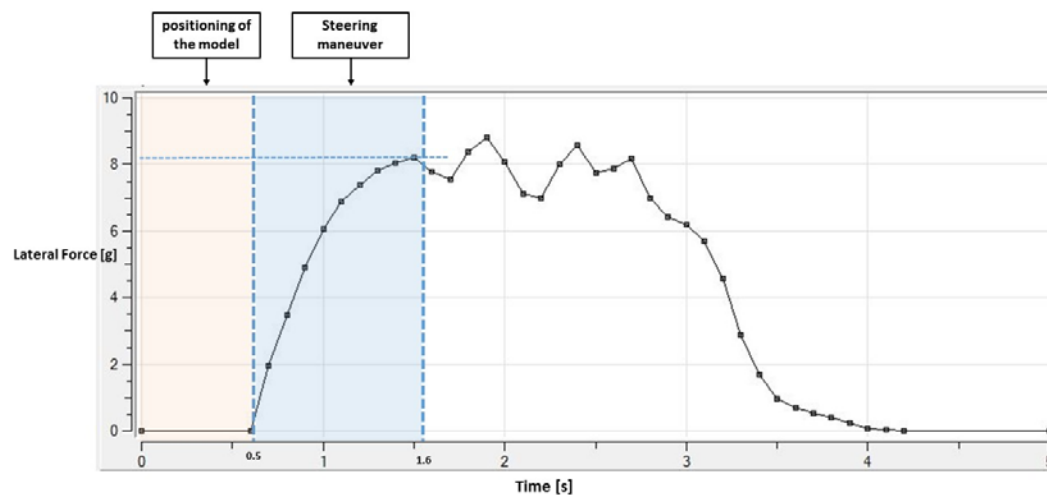


*Fig. 8 Pulse used to simulate the steering event, a lateral acceleration of 0.8 g from [4]. The first 0.500 s was to position the model. The simulation ended at 1.600 s, hence only the beginning of the steering event was simulated.*

Version 32 of the active 6-year-old HBM [8] was used as a baseline, modifying the definition of the angles used to calculate the error for the PID control (see Table 1 and Appendix A). Three different options were implemented:

**Option 1**, the spinal joint angles were measured by taking the angle of the inferior vertebra relative to the superior vertebra: Sacrum-L5, L5-L4, L4-L3, L3-L2, and etcetera.

**Option 2**, the lumbar joint angles were measured by taking the vertebral angle relative to the pelvis, while the thoracic and cervical joint angles were measured by taking the vertebral angle relative to the global coordinate system (floor of the vehicle). Vertebrae from L5 to L1 were referenced to the pelvis, while from the vertebrae T12 to C1 were referenced to the global coordinate system.

**Option 3**, all spinal joints were measured by taking the vertebral angle relative to the global coordinate system (floor of the car), from the vertebrae L5 to the C1.

Table 1 List of all models used to simulate the steering event. Time constants were:  $T_i=1$  s &  $T_d=0.1$  s. The hip control gains were: 37.5, 10, and 37.5 Nm/rad for flexion-extension, lateral bending, and rotation, respectively. In all the models, the hip angle was measured relative to the pelvis. For all the situations, the model was seated on a booster and restraint with a 3 points seatbelt. \*Indicate ranges used for the sensitivity study.

|                | Joint angle measured relative to                             | Cervical spine proportional gains [Nm/rad] |                          |                   | Thoracic spine proportional gains [Nm/rad] |                          |                   | Lumbar spine proportional gains [Nm/rad] |                          |                   | Hand tied to booster |
|----------------|--|--|--------------------------|-------------------|--|--------------------------|-------------------|--|--------------------------|-------------------|----------------------|
|                |  | Flexion-extension (KC)                     | Lateral Bending (KC_lat) | Rotation (KC_rot) | Flexion-extension (KT)                     | Lateral Bending (KT_lat) | Rotation (KT_rot) | Flexion-extension (KL)                   | Lateral Bending (KL_lat) | Rotation (KL_rot) |                      |
| Version 32     | Pelvis   | 10   | 10                       | 10                | 25   | 25                       | 25                | 37.5                                     | 37.5                     | 37.5              | Yes                  |
| Option 1       | Vertebrae  | 10   | 10                       | 10                | 25   | 25                       | 25                | 37.5                                     | 37.5                     | 37.5              | Yes                  |
| Option 2       | Lumbar spine → Pelvis<br>Thoracic & Cervical spine → Vehicle | 10   | 10                       | 10                | 25   | 25                       | 25                | 37.5                                     | 37.5                     | 37.5              | Yes                  |
| Option 3       | Vehicle  | 10   | 10                       | 10                | 25   | 25                       | 25                | 37.5                                     | 37.5                     | 37.5              | Yes                  |
| In ref [7]     | Vehicle  | 4  | 4                        | 4                 | 30   | 30                       | 30                | 45                                       | 45                       | 45                | No                   |
|                |  |  |                          |                   |  |                          |                   |  |                          |                   |                      |
| Optimization 1 | Vehicle  | 2-15*                                      | 2-15*                    | 10                | 15-40*                                     | 15-40*                   | 25                | 40-50*                                   | 40-50*                   | 37.5              | Yes                  |
| Optimization 2 | Vehicle  | 2-12*                                      | 2-12*                    | 10                | 19-29*                                     | 19-29*                   | 25                | 32-40*                                   | 32-40*                   | 37.5              | Yes                  |

## 4.2 Sensitivity

The optimization package LS-OPT (LSTC, California, USA) was used to study the sensitivity of the gains. Data was post-processed using MATLAB (v. R2010b) (The MathWorks, Inc., Massachusetts, USA). **Option 3** (see Table 1) was used as baseline of the active 6-year-old HBM. The strategy followed was a single iteration generating 43 different models with random gain values, between the defined ranges. The sampling was carried out using a Meta Model radial basis function, where the point selection was done by space filling.

The bounded variables were the proportional gains for flexion-extension and lateral bending rotational degrees of freedom for the lumbar, thoracic, and cervical spine (see Table 1). To simplify, the gains for the axial rotational degrees of freedom were not taken into account.

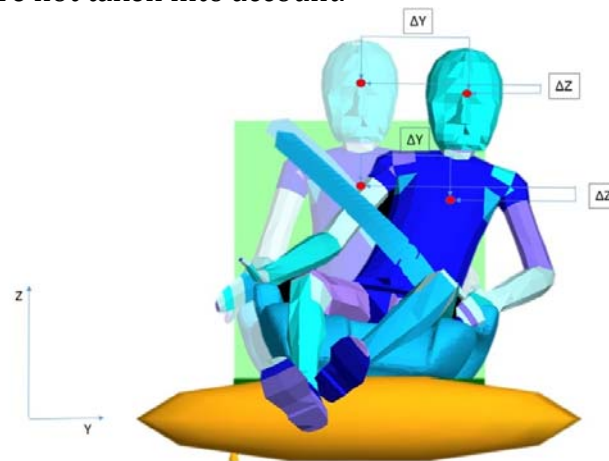


**Fig. 9** Nodes used to measure the displacement of the nasion and the upper sternum.

Output was the maximum displacement in the global Y and Z directions for two nodes: the nasion (node number: 52047) and the upper sternum (node number: 68000) (see Fig. 9). Finally, the goal of the sensitivity study was to determine how the different controller gains changed the displacement of the active 6-year-old HBM compared to the average volunteer data. The measured displacements were the differences between the simulated and experimental positions of the nasion and upper sternum nodes (Fig 9). The comparisons were done when the simulation time was 1.1 s (noted as an asterisk in Fig. 10). The average volunteer positions are marked in Fig. 10 with a cross for the nasion displacement and with a dotted line for the upper sternum displacement.

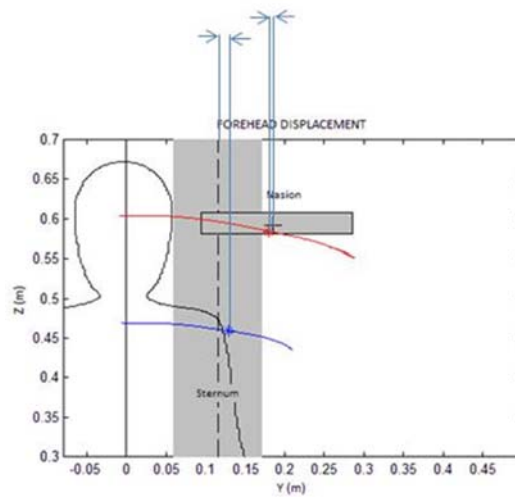


Fig. 10 The objective of the optimization was minimized the distance between the average volunteer data [4] and the displacement of the active 6-year-old HBM (Option 3) at 1.1 s during the steering event.

## 5 Results

### 5.1 Simulation

#### 5.1.1 Active 6-year-old HBM version 32

The active 6-year-old HBM version 32 nasion and upper sternum nodal trajectories are shown in Fig. 11. The position of the active 6YO HBM at 1.1 s was marked with an asterisk. This position correlates to the volunteer data taken at 0.6 s in the experiments. The range of displacement for the volunteer data are defined with dark grey areas, where the dashed line marks the average of these values for sternum Y-shifts and the cross marks the average for nasion displacement. If the asterisk (\*) is within the limits, the model resembles the volunteer kinematics, and thus it could be concluded that the model is relatively biofidelic.

Version 32 has a longer displacement along the Y axis (as shown in Fig. 11), compared to the other models proposed. The difference between the model's displacement of the upper sternum node compared to the average volunteer displacement (dotted line situated at 0.116 m from the initial position in the Y-axis) is approximately 0.013 m (Table 2). The displacement for the forehead of this version of the 6-year-old HBM is the closest value to the average volunteer displacement, 0.1799 m (Table 2). Both the asterisks for the displacement of the head and the displacement for the upper sternum are within the boundaries, then, this version of the active 6YO HBM resembles a biofidelic behavior. Fig. 12 shows a straight spine leaning to the side, due to the fact that the angles of joints of the vertebrae are measured relative to the pelvis. The pelvic and the body tilt to the side is as a result of a combination of the acceleration loading, acting on the center of mass of the upper body, and the interaction between the lap belt and leg.

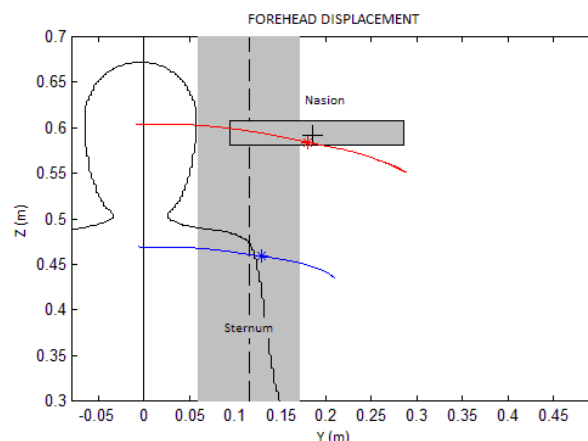


**Fig. 11** Trajectories for nasion and upper sternum in the active 6-year-old HBM Version 32, where the grey corridors are the range of volunteer data [4] at 1.1 s (\* in simulation trajectory).

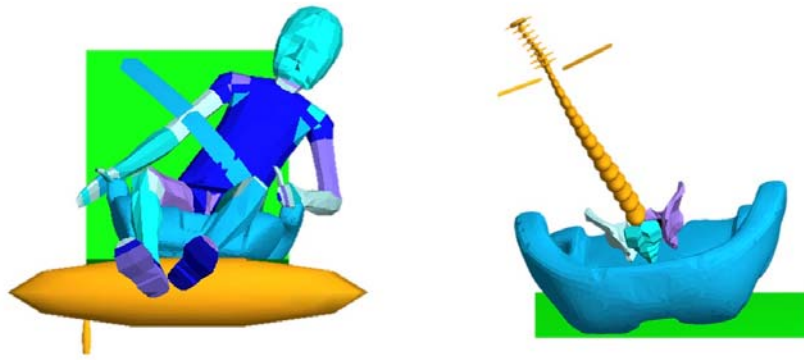


Fig. 12 Front view of the whole model with the active 6-year-old HBM version 32 (left) and a back view of the spine (right) at 1600ms in the simulation.

### 5.1.2 Head and upper sternum displacements

The averages for the nasion and sternum Y- displacement, obtained from the volunteer data after 0.6s of steering event, correspond with 0.185 m for the head displacement and 0.116 m for sternum. While the displacements of the three versions of the active 6-year-old HBM at 1.1 s of simulation are shown in Table 2.

Table 2 The nasion and sternum Y-displacements at 1.1 s for three versions of the active 6-year-old HBM.

|                         | Displacement at 1.1 s of simulation |                        |
|-------------------------|-------------------------------------|------------------------|
|                         | Nasion node (m)                     | Upper Sternum node (m) |
| Version 32<br>(ref [8]) | 0.1799                              | 0.1292                 |
| Option 2                | 0.1544                              | 0.1347                 |
| Option 3                | 0.1476                              | 0.1252                 |

### 5.1.3 Kinematic responses

After running the simulation with the active 6-year-old HBM Options 1-3, it was necessary to discard Option 1, where the vertebral angle was measured relative a neighboring vertebra(see Table 1), as a result of unnatural behavior. During the first 0.500 s, which is the time where just the gravity load is applied, the version of the active 6YO HBM was not maintaining a stable posture. Its neck and head turned mainly in rotation (see Fig. 13). For that reason, this unstable model was discarded.

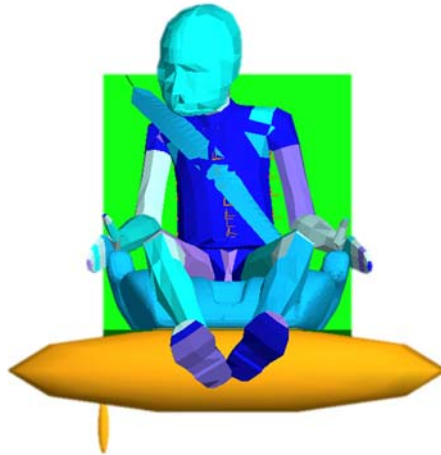


Fig. 13 Front view of the active 6-year-old HBM Option 1 at 500 ms where just the gravity acceleration was applied.

Fig. 14 illustrates the motion of the active 6-year-old HBM **Option 2** (see Table 1), where the joints of the cervical and thoracic spine were referenced to a global coordinate system (floor of the car) and the lumbar vertebrae were referenced to the pelvis, in the steering simulation.

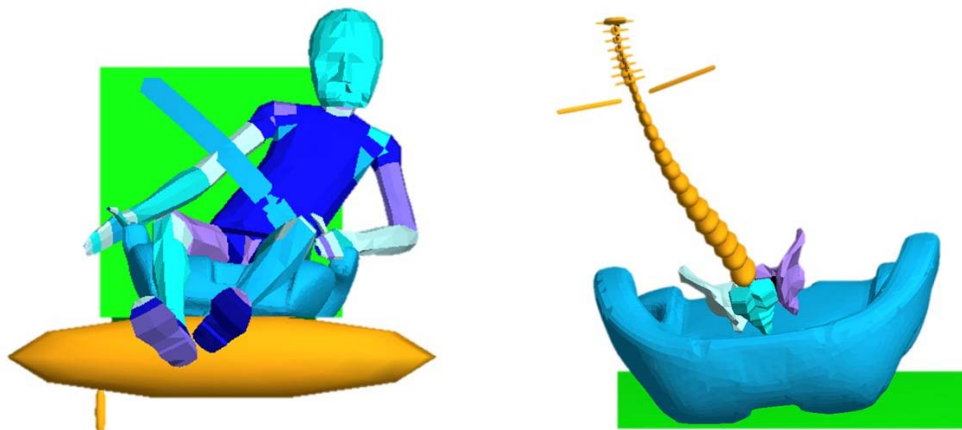


Fig. 14 Front view of the active 6-year-old HBM Option 2 (left), and back view of the spine (right) in the steering simulation at 1.6 s.

The trajectory of the nasion node and upper sternum node show that only a fraction is within the corridors, however, both the displacement for the head and the upper sternum at 1.1 s of simulation (marked by an asterisk in Fig.15), are within the corridors. It means that this model has a biofidelic behavior. However, the displacement for the upper sternum is the furthest from the average for the volunteer data between the models tested; it is at a distance of 0.018 m from the dashed line (Fig. 15). Fig. 14 illustrated the maximum displacement for the active 6-year-old HBM Option 2.

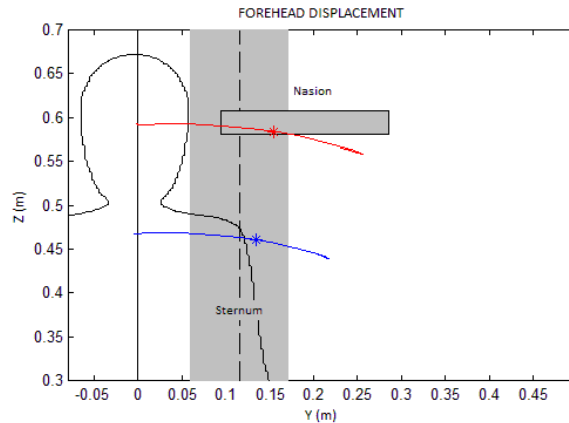


Fig. 15 Trajectories for nasion and upper sternum in the active 6-year-old HBM Option 2, where the grey corridors are the range of volunteer data [4] at 1.1 s (\* in simulation trajectory)..

Finally the trajectories of the nasion and upper sternum nodes for the active 6-year-old HBM **Option 3** (see Table 1), indicate that the model's responses are within the experimental ranges (see Fig. 17). The displacement for the sternum along the Y-axis exceeded in 0.009 m the average of the volunteer data (Table 2). The simulation of the maximum displacement with this model is illustrated in Fig. 16.

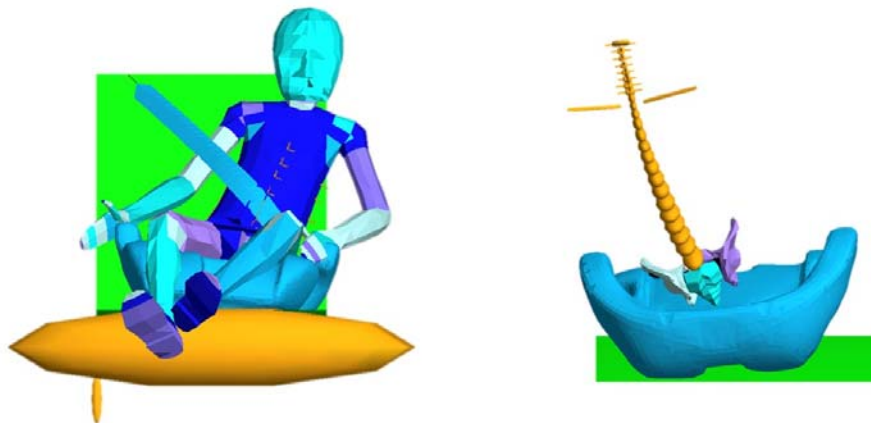


Fig. 16 Front view of the active 6-year-old HBM Option 3 (left), and back view of the spine (right) in the steering simulation at 1.6 s.

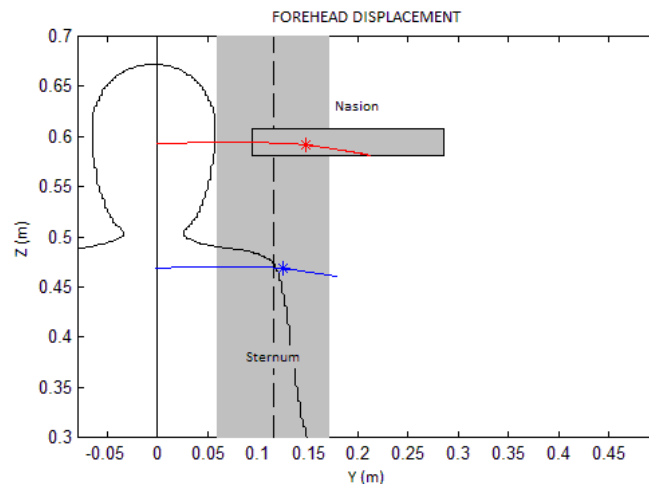


Fig. 17 Trajectories for nasion and upper sternum in the active 6-year-old HBM Option 3, where the grey corridors are the range of volunteer data [4] at 1.1 s (\* in simulation trajectory).

After comparing the options proposed, the model chosen to continue working with in the next part will be the model where the vertebrae are referenced to the global coordinate system, active 6-year-old HBM **Option 3**.

## 5.2 Sensitivity

The results obtained by LS-Opt (LSTC, California, USA) in Optimization 1 and Optimization 2 (see Table 1) are shown respectively in Fig. 18 and Fig. 19. These graphs show the influence of each gain (left side of the chart) on the displacement along the Y and Z-axis for two nodes; the nasion and the upper sternum. The ranges of displacements at 1.1s for all simulations performed are represented in Table 3. In addition to that, the displacement of the sternum along the Z-axis is not taken into account because the Z-values change between the different simulations less than 9 mm (Table 3). The same reason is applicable, when it comes to nasion displacement along the Z-axis. Even if the gains varied, the results of the different trajectories obtained deriving from the gain change itself would only imply a displacement range of 1 cm (Table 3). Thus, the importance of the gain values are marginal, and therefore the results from the sensitivity study will focus on the Y-values.

**Table 3 Range for the values of the displacement, for the results of the sensitivity study. The values are the maximum and minimum Y and Z displacements at 1.1 s.**

|                | Nasion node (m)   |                   | Upper Sternum node (m) |                   |
|----------------|-------------------|-------------------|------------------------|-------------------|
|                | Y-axis            | Z-axis            | Y-axis                 | Z-axis            |
| Optimization 1 | 0.1235-<br>0.1709 | 0.5902-<br>0.6004 | 0.1057-<br>0.1292      | 0.4674-<br>0.476  |
| Optimization 2 | 0.1405-<br>0.1762 | 0.5878-<br>0.5991 | 0.1205-<br>0.1359      | 0.4653-<br>0.4736 |

The results represented in both figures (Fig. 18-19) indicate that the gains for the thoracic and lumbar spine for the flexion-extension rotational degree of freedom (KT and KL) are not influential in the steering event. The sensitivity study shows that the most influential gains in the steering event are the gains corresponding with the cervical, thoracic and lumbar spine for lateral bending. However, in optimization 1 (Fig. 18) the KT\_lat gain has most influence, while in optimization 2 (Fig. 19) the KL\_lat gain has most influence.

As far as the nasion goes, Fig. 18 and Fig. 19 bring out a disagreement as for which is the most influential gain. Fig. 18 suggests that KT\_lat is the most influential, while KC\_lat is the most influential gain from the nasion in Fig. 19. This is because in Optimization 1 (Fig.18), the ranges of values for the thoracic spine were large (Table 1). Due this, changing the values for the gains of the thoracic spine had more influence for the displacement of the head and the response of the spine. Nonetheless, in the Optimization 2 (Fig.19) the boundaries for the thoracic spine were lower, decreasing all the influence of the

displacement of the head on the gains of the cervical spine. However, for the nasion node it can be concluded that lateral bending gains were the most influential.

When it comes to thoracic displacement along the Y-axis, both figures coincide in suggesting that the most influential gains are those, which correspond to lumbar spine (KL\_lat) and thoracic spine (KT\_lat). However, Fig. 18 points to the fact that the thoracic spine gain is the most influential, while Fig. 19 points to the lumbar spine. The reason can be that the values of the boundaries for the lumbar spine were higher in Optimization 1 (Fig. 18) than Optimization 2. The high KL\_lat gains provided a stiff response and therefore the lumbar spine was straighter than the thoracic spine, making the sternum displacement depend mainly on the gains for the thoracic spine. Whereas, in Optimization 2 (Fig.19), the values for the boundaries of the lumbar spine were lower (Table 1), increasing the influence of lumbar gain.

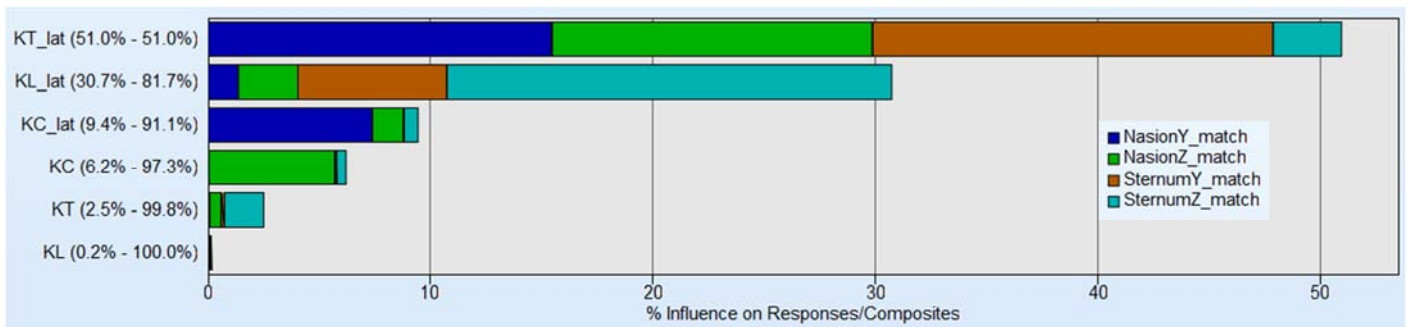


Fig. 18 Sensitivity plot for the first range of values for the variables, each bar shows the influence of the gains for each displacement proposed in the model Optimization 1.

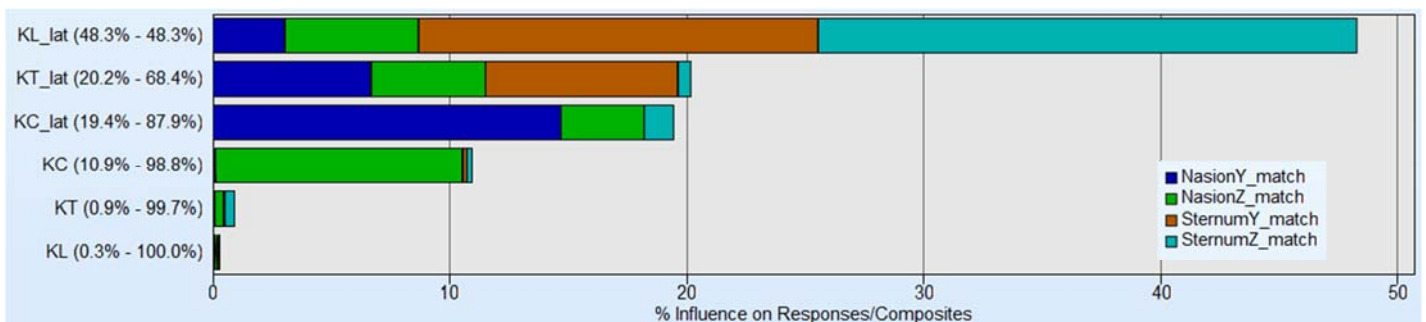


Fig. 19 Sensitivity plot for the second range of values for the variables, each bar shows the influence of the gains for each displacement proposed in the model Optimization 2.

## 6 Discussion

Trying to understand how changing the joint reference angle, that provides input to a PID controller and measures the rotation of vertebrae, affect model response, in this case, an active 6-year-old HBM [8], several models were suggested. These models were compared to the response measured in tests where child volunteers participated [4]. In these tests, proprioception and balance-maintenance were the notions in charge of modifying body posture as a response to different emergency events, so as to maintain an upright sitting position [14][15].

This thesis' result shows how the angle of the vertebrae that are measured relative to the global coordinate system, such as the vehicle floor, provide an input to the active muscle torques applied. It can indeed be a valid approach to predict child kinematics, as well as a 6-year-old HBM that could be used for future research and development of safety systems.

However, there are some limitations. By definition, a model approximates reality. In this case, the chosen active 6-year-old HBM seems to be appropriate to study a child's kinematic response during pre-crash events, in particular, steering and braking. It might be appropriate to study other situations as well. However, this cannot be supported by the research that falls under the scope of this thesis.

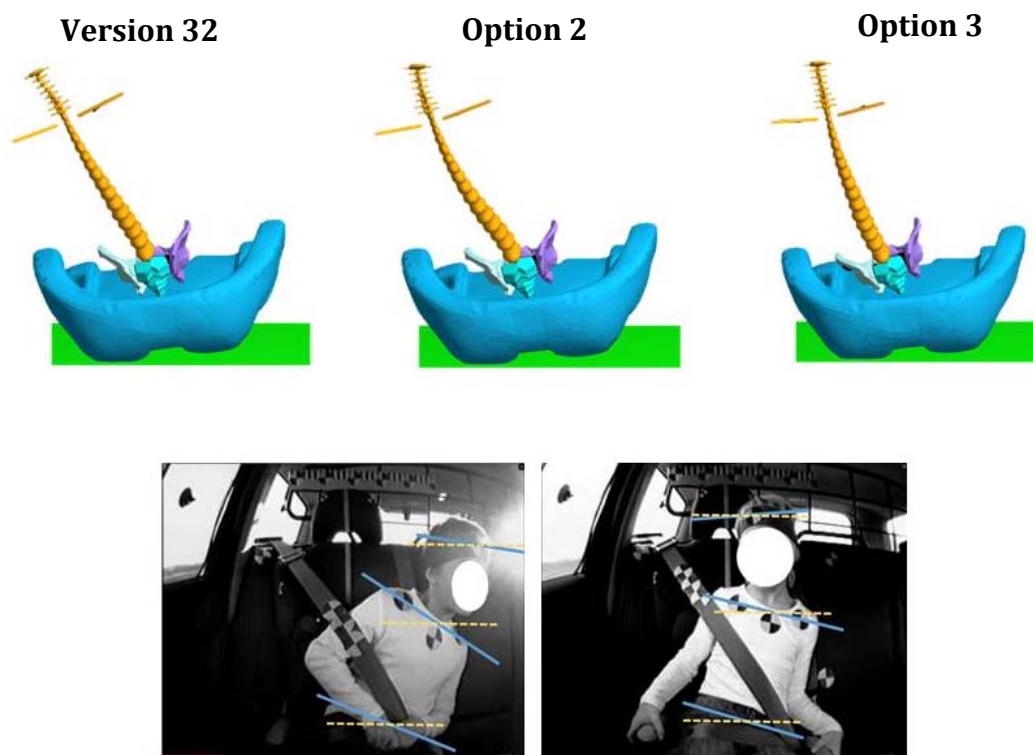


Fig. 20 Simulation of the different version of the active 6-year-old HBM. From left to right at the top, version 32, where the joints angles are relative to the pelvis; Option 2, where the lumbar angles are relative to the pelvis while the other spinal angles are relative to a global system; Option 3, where all spinal angles are relative to a global system. At the bottom, two photos taken from the experimental data with child in steering event [4] are supplied for comparison.

The human body keeps its balance with three separate systems [18] that can explain the child's kinematic responses. The first system is the vestibular system in the inner ear, containing the semicircular canals, which informs the brain about the movement of the body [19]. This may explain why the children try to keep the head parallel to the ground. The second system consists of the eyes, which create an image analyzed by the brain to understand what the position of the body is [19]. This justifies why the children move their heads, trying to watch across the front window and in some cases across the lateral window as well, to gain awareness of what is happening. The third system is the proprioception; in the muscles, joints and ligaments of the body there are strain sensitive receptors to inform the brain where the body is in each moment with respect to the external environment [19]. This is the main reason to explain why the children react trying to keep their initial position.

To determine which version (v32, Option2 or Option 3) that has the most biofidelic behavior, the simulation data was compared to the volunteer data [4] in terms of the displacement of the head and the sternum, comparing the trajectory of each model with the corridors set by the volunteer data. Version 32 had a lot of displacement and never, even when the gains were tuned, did the trajectory follow the same trend. Because of this, the gains just increased or decreased the stiffness of the spine, but not its shape. In this case, the behavior of this model is due to the interaction between the lap belt and leg. This interaction in combination with the acceleration loading, acting on the center of mass of the upper body, creates the pelvic tilt and makes the body tilt to the side.

The decision to include an active 6-year-old HBM with the reference system that Option 2, where the joints of the cervical and thoracic spine are referenced to a global coordinate system (floor of the car) and the lumbar vertebrae joints are referenced to the pelvis, was based on physiology. Since the pelvis is restrained by the lap belt, it made sense to think that the lower part of the spine would be related to the inclination of the pelvis. The rest of the spine would, in theory, be in charge of bringing the body back to its initial position, helped of course by the musculature. However, even though Option 2 followed what was initially perceived as a sound rationale, the simulations proved this to not be the case. For this model, the pelvis does not always remain in the same position. Therefore, the lumbar spine is straighter than the thoracic and cervical spine that are referenced to the floor. Consequently, the lower back had a much straight response (as it depended on the pelvis' movements) and could aid the middle and higher regions of the spine compensate lateral movements.

Option 3 was the active 6YO HBM that had the most biofidelic behavior. As explained earlier, its trajectories were inside the corridors of the volunteer data. It is the model that most closely resembles the response of a child that would undergo the same events the model was exposed to.

At this point, it is essential to remember that the active 6-year old HBM is a model. While the role of this model is to represent child kinematic responses during steering and braking events, that does not mean it can be used for

everything. Thus, it has its limitations. For instance, it may not be an appropriate model to study injury predictions or muscle tensions in a car crash situation. In order to do that, the active 6YO HBM would need a thorough validation in the crash loading regime to know if the results obtained are sufficiently good or otherwise insufficient. Furthermore, this active 6-year-old HBM could not be useful to simulate the kinematic response as a pedestrian, due to the fact that neither the arms nor the legs have controller implementation to have an active articulations to resemble a biofidelic behavior.

The lateral force applied makes the child move the center of gravity of her or his body to the left. As a consequence, the child applies weight to the left side, making the pelvis tilt slightly. At the same time, it makes the booster rise, even if the pelvis is retained by the lap belt. Hence, it is important to consider at this point that the contact between the booster and the child and/or the seat and the booster might be different in reality. It may be the case that friction between the child and the booster is larger than assumed, or that the booster stays still due to its being anchored to the seat.

One of the problems found was that specific factors in the kinematic response of the children could not be collected by the volunteer data due to the fact that neither the tilt of the pelvis nor the shape of spine were measured. Visually, it is impossible to say which one is the best model, because the data is not enough. To illustrate this point, taking Fig. 20 as an example, the behavior of the child to the right seems to be accurately depicted by the shape of the spine in Option 3, while the shape of the spine of Version 32 looks like the child on the left. Meanwhile, the tilt of the pelvis in Version 32 is similar to the pelvis' position of the child to the right, whereas the inclination of the pelvis for Option 3 seems to correspond to the child in the left photo. As one can see, many model positions *seem* to reflect different parts of the picture but, without data, it cannot be stated that those model positions represent exactly what is going on in the picture. That being said, and bearing the data in mind, the most biofidelic model out of those tested was **Option 3**.

The displacement of the active 6-year-old HBM [8] along the Z-axis does not appear to be influential during the steering event. This makes sense, since the movement that the body can do along this axis during lateral acceleration is reduced. The range of displacement along the Z-axis for the model is around 0.5cm in all simulations, almost insignificant compared to displacement along the Y-axis. Meanwhile, the displacement along the Y-axis seemed to have more influence when lateral force was applied, due to the fact that the seatbelt restraint the movements along the Z and X axes. Due to this, the most influential gains during the steering event are the gains for lateral bending for the lumbar, thoracic, and cervical spine. The most influential gain, according to the research conducted in this thesis, was the thoracic gain for lateral bending. This was due to the fact that this gain directly affects displacements of both the sternum and the head.

Knowing the kinematic response of a child and his or her body in pre-crash situations, and creating a model that is biofidelic can help to prevent injuries in vehicle crashes that are influenced by a pre-crash scenario. Exposing

actual volunteers to such events can be, even with different restraint systems, extremely dangerous. However, having a biofidelic model can throw a lot of light upon data regarding kinematic responses in pre-crash situations, actual effectiveness of different restraint systems, as well as a wide array of applications that eventually make complex design and testing processes more efficient, effective, and cheap, and less time-consuming. Even though this model has, as any other does, its limitations, it was found to be biofidelic enough so as to create baseline projections of how a child's body might move during steering and braking events.

This thesis has sought to contribute to our understanding of the kinematic responses and characteristics of this active 6-year-old HBM, as well as to gain a better understanding of the model, after lateral acceleration is applied. It is useful, however, to understand and keep in mind the scope of model, so that the situations and events in which the model itself is relevant and therefore applicable are clear to its potential users.

## 7 Conclusion

The active 6-year-old HBM, with vertebral angles measured relative to the global coordinate system (**Option 3** model), is quite biofidelic. Because the movement of the spine in the model *resembles* what could easily be the spine movement of a real child, if he or she were to be subjected to the kind of loads applied in the testing of the model. Furthermore, the displacement for the head and sternum of the 6-year-old HBM after 1.1s simulation are within the corridors created by the position of the volunteers after 0.6s steering event.

In the steering event, the sensitivity study showed that the gains with the largest influence on displacements along the Y-axis were gains involved in lateral bending for cervical, thoracic and lumbar parts. At this point, it is important to stress that cervical and thoracic gains influence displacements of the head, and lumbar gains effect the displacement of the sternum.

## 8 Future Work

A possible field of application for the active 6-year-old HBM, as it is now, could be to improve the 3-point seatbelt used to restraint the child or the assessment of the influence for different child seats in the child's kinematic response.

Possible future research might consist of adding controller implementation in the active 6-year-old HBM's arms to reproduce the force created by some children, in cases where arms are used to recover the initial position. In addition to that, it would be interesting to test the responsiveness of the model in different events, so as to verify the biofidelity of the model for a larger range of loading conditions. For instance, events with large oscillations, combined evasive events (braking-steering event), passenger ergonomics, etcetera. Moreover, testing the model with different boosters to know how affect to the behavior of the child and also testing different new restraint technology, such as the pre-pretension seat belt.

Finally, more data sampling would be useful to better understanding the kinematic response of children. This would be of use when it comes to designing new models, as researchers would have a more accurate idea of certain behaviors that are outside normal distributions.

## 9 References

- [1] MADYMO Human Models Manual Release 7.4.1, (2012). TAN/TASS, Rijswijk, the Netherlands.
- [2] Mitis, F., & Sethi, D. (2013). *European facts and global status report on road safety 2013*. World Health Organization, Regional Office for Europe.
- [3] World Health Organization. (2013). *WHO global status report on road safety 2013: supporting a decade of action*. World Health Organization
- [4] Bohman, K., Stockman, I., Jakobsson, L., Osvalder, A. L., Bostrom, O., & Arbogast, K. B. (2011, October). Kinematics and shoulder belt position of child rear seat passengers during vehicle events. In *Annals of Advances in Automotive Medicine/Annual Scientific Conference* (Vol. 55, p. 15). Association for the Advancement of Automotive Medicine.
- [5] Stockman, I., Bohman, K., Jakobsson, L., & Brodin, K. (2013). Kinematics of child volunteers and child anthropomorphic test devices during emergency braking events in real car environment. *Traffic injury prevention, 14*(1), 92-102.
- [6] Andersson, M., Bohman, K., & Osvalder, A. L. (2010, January). Effect of booster seat design on children's choice of seating positions during naturalistic riding. In *Annals of Advances in Automotive Medicine/Annual Scientific Conference* (Vol. 54, p. 171). Association for the Advancement of Automotive Medicine.
- [7] Brodin, K., Stockman, I., Subramanian, H., Öst, J., & Gras, L. L. (2015) Development of an Active 6-Years-Old Child Human Body Model for Simulation of Emergency Events. Chalmers University of Technology, Göteborg, Sweden & Indian Institute of Technology, Delhi, India.
- [8] Brodin, K., Gras, L. L., & Stockman, I. (2014). Active spine modeling representing a 6 year-old child. In *7th World Congress of Biomechanics* (No. 16-14).
- [9] Burdi, A. R., Huelke, D. F., Snyder, R. G., & Lowrey, G. H. (1969). Infants and children in the adult world of automobile safety design: pediatric and anatomical considerations for design of child restraints. *Journal of Biomechanics, 2*(3), 267-280.
- [10] Kasai, T., Ikata, T., Katoh, S., Miyake, R., & Tsubo, M. (1996). Growth of the cervical spine with special reference to its lordosis and mobility. *Spine, 21*(18), 2067-2073.
- [11] Arbogast, K. B., Balasubramanian, S., Seacrist, T., Maltese, M. R., Garcia-Espana, J. F., Hopely, T., ... & Higuchi, K. (2009). Comparison of kinematic

responses of the head and spine for children and adults in low-speed frontal sled tests. *Stapp car crash journal*, 53, 329.

- [12] Brolin, K., Stockman, I., Andersson, M., Bohman, K., Gras, L. L., & Jakobsson, L. (2015). Safety of children in cars: A review of biomechanical aspects and human body models. *IATSS research*, 38(2), 92-102.
- [13] Razmjooy, N. (2014, Oct 09). PID control. In Math works. Retrieved June 14, 2015. From <http://www.mathworks.com/matlabcentral/fileexchange/48060-pid-control/content/PID.m>
- [14] Cappon, H., Mordaka, J., Van Rooij, L., Adamec, J., Praxl, N., & Muggenthaler, H. (2007). *A computational human model with stabilizing spine: a step towards active safety* (No. 2007-01-1171). SAE Technical Paper.
- [15] Liu, X. J., & Yang, J. K. (2002). Development of child pedestrian mathematical models and evaluation with accident reconstruction. *Traffic Injury Prevention*, 3(4), 321-329.
- [16] Gras, L. L., & Brolin, K. (2012). *Active Child Models for Traffic Safety Research, Interim Report 1, October 2012*. Chalmers University of Technology.
- [17] Brolin, K., & Gras, L. L. (2014). *Active Child Models for Traffic Safety Research Interim Report 2, October 2013*.
- [18] Foudriat, B. A., Di Fabio, R. P., & Anderson, J. H. (1993). Sensory organization of balance responses in children 3–6 years of age: a normative study with diagnostic implications. *International Journal of Pediatric Otorhinolaryngology*, 27(3), 255-271.
- [19] Grace Gaerlan, M., Alpert, P. T., Cross, C., Louis, M., & Kowalski, S. (2012). Postural balance in young adults: the role of visual, vestibular and somatosensory systems. *Journal of the American Academy of Nurse Practitioners*, 24(6), 375-381.

# 10 Appendix

## 10.1 Appendix A

Code used to modify the reference point. The code was created by Gras and Brolin [16-17] and the name of the file is PID6YO\_v19.xml, where the part where the change was done is the definition of the sensor for Y-rotation, X-rotation and Z-rotation. Due to the extension of the code, only certain parts – considered relevant – are presented. They seek to show the methodology followed for each option proposed:

### Option 1

```
<COMMENT>
<![CDATA[===== Sensors for Y-rotation =====]]>
</COMMENT>
<SENSOR.BODY
  ID="61002"
  VECTOR="0 1 0"
  SIGNAL_TYPE="ANG_DISP"
  NAME="Sacrum_sensor"
>
  <POINT_OBJECT_1.MB
    BODY="Pelvis_bod"
    POS="0.1 0.0 0.0"
  />
</SENSOR.BODY>
<SENSOR.BODY_REL
  ID="61028"
  SIGNAL_TYPE="ANG_DISP"
  NAME="HipR_sensor"
>
  <POINT_OBJECT_1.MB
    BODY="Pelvis_bod"
    POS="0 -0.1 0"
  />
  <POINT_OBJECT_2.MB
    BODY="LegUpR_bod"
    POS="0.1 0 0"
  />
</SENSOR.BODY_REL>
<SENSOR.BODY_REL
  ID="61029"
  SIGNAL_TYPE="ANG_DISP"
  NAME="HipL_sensor"
>
  <POINT_OBJECT_1.MB
    BODY="Pelvis_bod"
    POS="0 -0.1 0"
  />
  <POINT_OBJECT_2.MB
    BODY="LegUpL_bod"
    POS="0.1 0 0"
  />
</SENSOR.BODY_REL>
<SENSOR.BODY_REL
  ID="61003"
  SIGNAL_TYPE="ANG_DISP"
  NAME="Sacrum_L5_sensor"
>
  <POINT_OBJECT_1.MB
```

```

    BODY="Pelvis_bod"
    POS="0 -0.1 0"
  />
  <POINT_OBJECT_2.MB
    BODY="L5_bod"
    POS="0.1 0 0"
  />
</SENSOR.BODY_REL>
<SENSOR.BODY_REL
  ID="61004"
  SIGNAL_TYPE="ANG_DISP"
  NAME="L5_L4_sensor"
  >
  <POINT_OBJECT_1.MB
    BODY="L5_bod"
    POS="0 -0.1 0"
  />
  <POINT_OBJECT_2.MB
    BODY="L4_bod"
    POS="0.1 0 0"
  />
</SENSOR.BODY_REL>
<SENSOR.BODY_REL
  ID="61005"
  SIGNAL_TYPE="ANG_DISP"
  NAME="L4_L3_sensor"
  >
  <POINT_OBJECT_1.MB
    BODY="L4_bod"
    POS="0 -0.1 0"
  />
  <POINT_OBJECT_2.MB
    BODY="L3_bod"
    POS="0.1 0 0"
  />
</SENSOR.BODY_REL>
<SENSOR.BODY_REL
  ID="61006"
  SIGNAL_TYPE="ANG_DISP"
  NAME="L3_L2_sensor"
  >
  <POINT_OBJECT_1.MB
    BODY="L3_bod"
    POS="0 -0.1 0"
  />
  <POINT_OBJECT_2.MB
    BODY="L2_bod"
    POS="0.1 0 0"
  />
</SENSOR.BODY_REL>
<SENSOR.BODY_REL
  ID="61007"
  SIGNAL_TYPE="ANG_DISP"
  NAME="L2_L1_sensor"
  >
  <POINT_OBJECT_1.MB
    BODY="L2_bod"
    POS="0 -0.1 0"
  />
  <POINT_OBJECT_2.MB
    BODY="L1_bod"
    POS="0.1 0 0"
  />
</SENSOR.BODY_REL>
<SENSOR.BODY_REL
  ID="61008"

```

```

SIGNAL_TYPE="ANG_DISP"
NAME="L1_T12_sensor"
>
<POINT_OBJECT_1.MB
  BODY="L1_bod"
  POS="0 -0.1 0"
/>
<POINT_OBJECT_2.MB
  BODY="T12_bod"
  POS="0.1 0 0"
/>
</SENSOR.BODY_REL>

```

## Option 2

```

<SENSOR.BODY_REL
  ID="61007"
  SIGNAL_TYPE="ANG_DISP"
  NAME="L2_L1_sensor"
  >
  <POINT_OBJECT_1.MB
    BODY="Pelvis_bod"
    POS="0 -0.1 0"
  />
  <POINT_OBJECT_2.MB
    BODY="L1_bod"
    POS="0.1 0 0"
  />
</SENSOR.BODY_REL>
<SENSOR.BODY_REL
  ID="61008"
  SIGNAL_TYPE="ANG_DISP"
  NAME="L1_T12_sensor"
  >
  <POINT_OBJECT_1.MB
    BODY="Pelvis_bod"
    POS="0 -0.1 0"
  />
  <POINT_OBJECT_2.MB
    BODY="T12_bod"
    POS="0.1 0 0"
  />
</SENSOR.BODY_REL>
<SENSOR.BODY_REL
  ID="61009"
  SIGNAL_TYPE="ANG_DISP"
  NAME="T12_T11_sensor"
  >
  <POINT_OBJECT_1.MB
    BODY="/Vehicle/FLOOR"
    POS="0 -0.1 0"
  />
  <POINT_OBJECT_2.MB
    BODY="T11_bod"
    POS="0.1 0 0"
  />
</SENSOR.BODY_REL>

```

.....

```

</SENSOR.BODY_REL>
<SENSOR.BODY_REL
  ID="61021"
  SIGNAL_TYPE="ANG_DISP"
  NAME="C7_C6_sensor"
  >
  <POINT_OBJECT_1.MB
    BODY="/Vehicle/FLOOR"
    POS="0 -0.1 0"
  />
  <POINT_OBJECT_2.MB
    BODY="C6_bod"
    POS="0.1 0 0"
  />
</SENSOR.BODY_REL>
<SENSOR.BODY_REL
  ID="61022"
  SIGNAL_TYPE="ANG_DISP"
  NAME="C6_C5_sensor"
  >
  <POINT_OBJECT_1.MB
    BODY="/Vehicle/FLOOR"
    POS="0 -0.1 0"
  />
  <POINT_OBJECT_2.MB
    BODY="C5_bod"
    POS="0.1 0 0"
  />
</SENSOR.BODY_REL>

```

### Option 3

```

<![CDATA[===== Sensors for Y-rotation =====]]>
</COMMENT>
<SENSOR.BODY
  ID="61002"
  VECTOR="0 1 0"
  SIGNAL_TYPE="ANG_DISP"
  NAME="Sacrum_sensor"
  >
  <POINT_OBJECT_1.MB
    BODY="/Vehicle/FLOOR"
    POS="0.1 0.0 0.0"
  />
</SENSOR.BODY>
<SENSOR.BODY_REL
  ID="61028"
  SIGNAL_TYPE="ANG_DISP"
  NAME="HipR_sensor"
  >
  <POINT_OBJECT_1.MB
    BODY="Pelvis_bod"
    POS="0 -0.1 0"
  />
  <POINT_OBJECT_2.MB
    BODY="LegUpR_bod"
    POS="0.1 0 0"
  />
</SENSOR.BODY_REL>
<SENSOR.BODY_REL
  ID="61029"
  SIGNAL_TYPE="ANG_DISP"
  NAME="HipL_sensor"

```

```

>
<POINT_OBJECT_1.MB
  BODY="Pelvis_bod"
  POS="0 -0.1 0"
/>
<POINT_OBJECT_2.MB
  BODY="LegUpL_bod"
  POS="0.1 0 0"
/>
</SENSOR.BODY_REL>
<SENSOR.BODY_REL
  ID="61003"
  SIGNAL_TYPE="ANG_DISP"
  NAME="Sacrum_L5_sensor"
>
<POINT_OBJECT_1.MB
  BODY="/Vehicle/FLOOR"
  POS="0 -0.1 0"
/>
<POINT_OBJECT_2.MB
  BODY="L5_bod"
  POS="0.1 0 0"
/>
</SENSOR.BODY_REL>
<SENSOR.BODY_REL
  ID="61004"
  SIGNAL_TYPE="ANG_DISP"
  NAME="L5_L4_sensor"
>
<POINT_OBJECT_1.MB
  BODY="/Vehicle/FLOOR"
  POS="0 -0.1 0"
/>
<POINT_OBJECT_2.MB
  BODY="L4_bod"
  POS="0.1 0 0"
/>
</SENSOR.BODY_REL>
<SENSOR.BODY_REL
  ID="61005"
  SIGNAL_TYPE="ANG_DISP"
  NAME="L4_L3_sensor"
>
<POINT_OBJECT_1.MB
  BODY="/Vehicle/FLOOR"
  POS="0 -0.1 0"
/>
<POINT_OBJECT_2.MB
  BODY="L3_bod"
  POS="0.1 0 0"

```